PERGAMON

Physics and Chemistry of the Earth 27 (2002) 1333–1341

PHYSICS and CHEMISTRY of the EARTH

www.elsevier.com/locate/pce

Magnetic properties of charcoal rich deposits associated with a Roman bath-house, Butrint (Southern Albania)

Mark W. Hounslow [a,*], Alex Chepstow-Lusty [b]

[a] CEMP, Department of Geography, Lancaster Environment Centre, Lancaster University, Lancaster LA1 4YW, UK
[b] Palèoenvironments & Palynologie, Case 61, ISEM, 3409S Montpellier, Cedex 05, France

Abstract

A section adjacent to a building structure at Shën Dëli, Butrint, Southern Albania exposes what is believed to be the remains of a former Roman bath-house. This section shows a transition from the underlying natural marsh clay into an archaeological deposit, which is both the basal remains of a building structure, and what appears to be an ash and charcoal enriched midden. The micro and macrocharcoal, magnetic and physical properties indicate a number of phases in the archaeological deposits, culminating in the micro and macrocharcoal rich and magnetically enhanced midden. The magnetic properties of these deposits are strongly related to the charcoal content that is probably a reflection of the ash content. The midden deposit is strongly enhanced in both superparamagnetic and low coercivity magnetite. The charcoal content and magnetic properties of the midden indicate a high content of wood-ash produced at the bath-house site, which is consistent with the anticipated fuel source for the region in Roman times.

Keywords: Microcharcoal; Superparamagnetism; Butrint; Magnetic properties; Wood burning

1. Introduction

Environmental magnetic measurements provide a variety of proxy data reflecting changes in both natural or anthropogenic induced inputs (Thompson and Oldfield, 1986; Dearing, 1999b). Such measurements may be sensitive to fire histories, because burning often produces elevated concentrations of magnetic minerals (Rummery, 1983; Kletetschka and Banerjee, 1995; Gedye et al., 2000; Ketterings et al., 2000). The reasons for this are twofold. First, combustion of fuel produces new magnetic minerals from the traces of Fe present within the fuel (Lu et al., 2000). Examples of this are the contamination of soils from fly ash, due to the combustion of coals in power stations (Petrovsky and Ellwood, 1999), and elevated magnetite concentrations in archaeological hearths (Peters et al., 2000). Second, the contact of fire with soils, produces new magnetic materials by heat conversion (Ketterings et al., 2000). These mechanisms have been suggested as factors for producing enhanced soil magnetic properties in natural environments subject to periodic burning (Kletetschka and Banerjee, 1995). Indications are that in some cases fire residues may be far more important than is commonly anticipated (Schmidt et al., 1999).

However, a more comprehensive database of magnetic properties associated with fired deposits needs to be developed, to better understand the characteristics of magnetic minerals produced by burning. This will enhance the usefulness of magnetic measurements in understanding archaeological and environmental deposits subject to fire. The aims of this study are to add to the mineral magnetic database by examining a case study from a charcoal rich deposit adjacent to a Roman bath-house. Assessment of the fire activity is based on the micro and macrocharcoal content of the deposits. Charcoal could potentially be natural or anthropogenic in origin (Patterson et al., 1987), but its association with adjacent archaeology indicates in this case, it is directly related to anthropogenic activity.

2. Butrint and its archaeology

The Butrint Park (a World Heritage site) has as its core a Hellenistic to late Roman city (Fig. 1). Its written history and archaeology is diverse and covered in Hodges et al. (1997) and Hodges et al. (2002). Beginning in Roman times the city spread out across the Vrina

* Corresponding author.
E-mail address: m.hounslow@lancaster.ac.uk (M.W. Hounslow).

1474-7065/02/$ - see front matter
PII: S1474-7065(02)00120-1

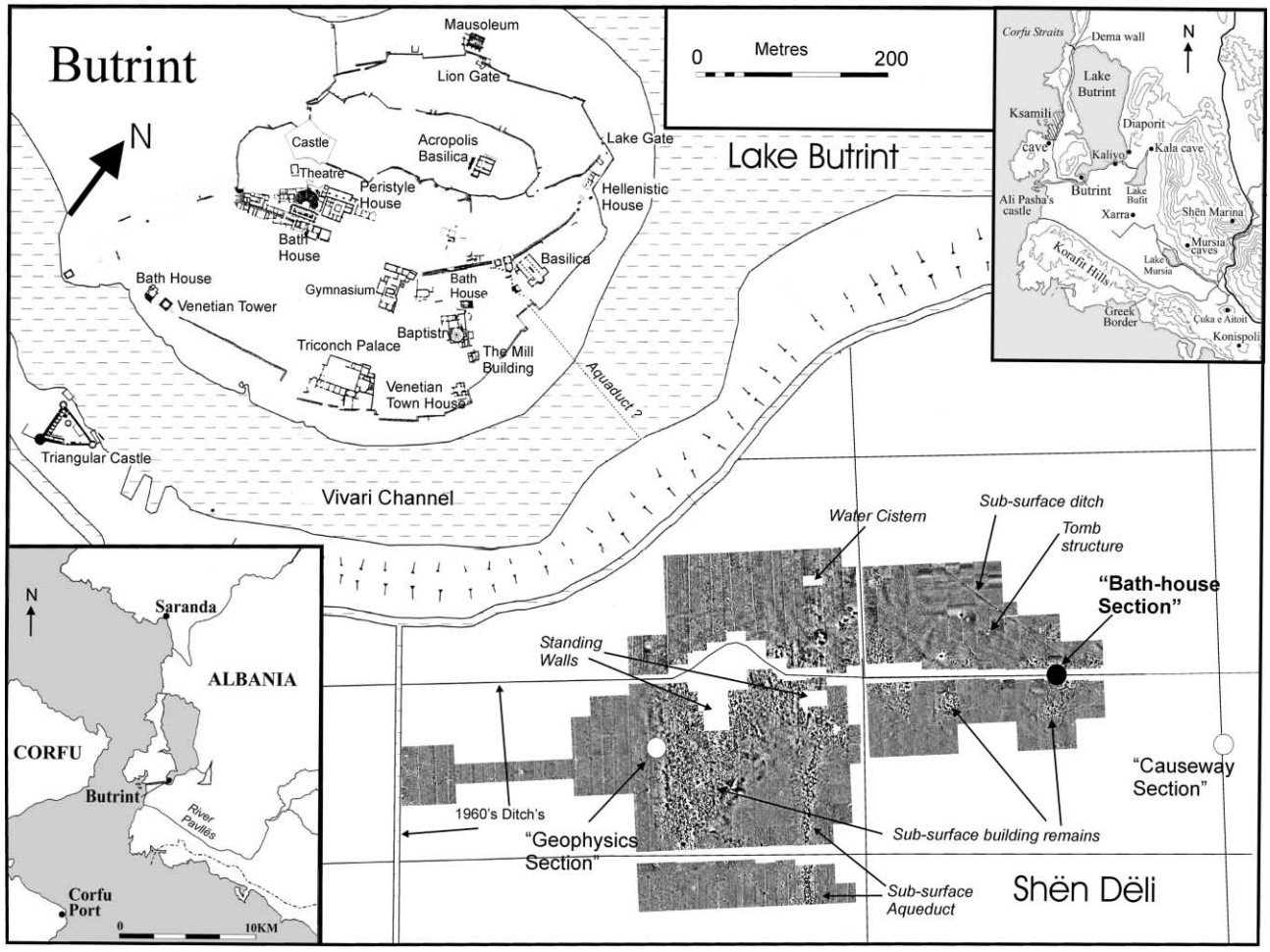

Fig. 1. Location of the Bath-house Sections used in this study (marked with black circle), and ancillary post-Roman sections (white circles). Their relationship to the archaeology and the magnetic gradiometer survey is indicated.

Plain, a marshy alluvial plain developing to the south. This plain is derived from the Pavllës River, which originates from the mountains to the east. The Vrina Plain has accumulated since the mid-Holocene in spite of a regional sea-level rise of between 0.4 and 0.9 mm/year since ca. 4000 BC, so that current sea-level is estimated to be 1–1.5 m higher than it was 2000 years ago (Hodges et al., 1997; Mathers et al., 1999). This rise in relative sea-level is evident in the flooded lower parts of the main Butrint site, and was a factor in the eventual abandonment of Butrint in late medieval times.

The Vrina Plain is currently reclaimed saltwater/brackish marsh, which was drained in the 1960s for agriculture. In the summer months spontaneous fires, or fires started by shepherds (to improve new growth for grazing) may occur on the plain or in the surrounding hilly grasslands. Historical records from the Roman period indicate that the region was extensively forested (Reale and Dirmeyer, 2000), although the time at which this ceased to be the case is unclear.

The Shën Dëli site, southeast of Butrint, has been shown by field walking and a magnetic gradiometer survey to contain extensive remains of Roman origin (Fig. 1). These are for the most part covered with 0.5–1.5 m of marsh clay (Hounslow and Chepstow-Lusty, 2002). Samples for analysis were collected from three sections on the Shën Dëli site (Fig. 1). These sections have been informally called, the Geophysics Anomaly Section, the Causeway Section and the Bath-house Section. The former two are principally sections through post-Roman natural marsh clay, whereas the Bath-house Section has archaeological horizons, adjacent to what has been interpreted as a Roman bath-house based on the presence of hypocaust tiles (Hodges et al., 1997). No formal archaeological excavations have currently taken place on the Shën Dëli site. This work primarily focuses on the Bath-house Section (Fig. 1).

3. Section details

The Bath-house Section is located in one of the 1960s NE–SW oriented drainage ditches, exposing the N–S aligned wall of a building. An array of N–S collinear

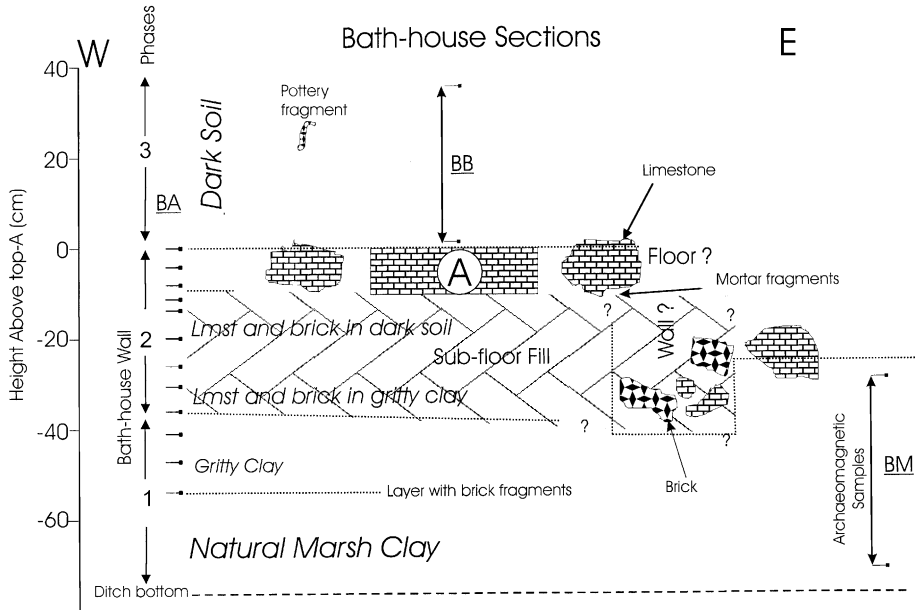

Fig. 2. Sketch of the stratigraphic details of the Bath-house Section. Sub-sections BA, BB and BM are indicated and their relationship to the features of the section. Horizontal scale approximate.

gradiometer anomalies are interpreted as a reflection of a regular wall or roadway alignment, of which the bath-house wall is a part (Chroston and Hounslow, 2002).

The section is external to the bath-house building, and the stratigraphy can be divided into three phases (Fig. 2):

- A lower interval of brown mottled, grey marsh clay (Phase 1). The N–S wall is built upon this clay. Near the top of this interval is a discontinuous layer of small brick fragments adjacent to the wall. The top of the interval near the bath-house wall (i.e. base of BA sub-section) is marked by ~13 cm of stiff gritty clay, which cannot be traced to the east of a vertical limestone/brick partition in the overlying phase.
- A middle interval (Phase 2), which is bounded at the top by a layer of limestone blocks (interpreted as a floor level, S. Martin, pers. comm. 1999), the most prominent block of which (labelled A) is used as a datum for the stratigraphy. This interval (adjacent to the bath-house wall only) is filled with limestone and brick rubble, with intervening clay (sub-floor fill?). The intervening clay between the blocks in the BA interval becomes darker coloured upwards. At sub-section BM to the east (in Phase 1), there is mostly marsh clay with occasional small pieces of brick in the uppermost part of the sub-section. The boundary between these east/west intervals is a short vertical partition (wall of pre-floor building?) of limestone and bricks.
- A black friable silty deposit (Phase 3), rich in small fragments of limestone and brick that rests on the limestone floor. A fragment of pottery was found in this interval, which may later provide a date. Without an archaeological excavation the precise origin of this deposit is uncertain but indications from this work, suggest it represents a midden, or occupation debris, external to the bath-house building.

The archaeomagnetic dating of samples from the lower part of sub-section BM (Phase 1, Fig. 2) was inconclusive (Hounslow and Chepstow-Lusty, 2002). There are two possible age matches, 200–400 AD interval, or 1800–1600 BC; the former being incongruent with the presumed age (ca. 2nd century AD) of the bath-house structure.

The Geophysics Anomaly and Causeway Sections preserve natural marsh clay sequences that rest on archaeological structures. Archaeomagnetic dating of the marsh clay in the Geophysics Section indicates that marsh clay growth over the rubble surface started between 450 and 500 AD, with 40 cm of marsh clay having accumulated by ca. 700–750 AD. In contrast, archaeomagnetic dating of the marsh clay at the Causeway Section indicates sedimentation was initiated between 800 and 850 AD. Extrapolation using sedimentation rates, indicates at both these sites, siltation to the present day soil surface occurred by ca. 1450–1600 AD (Hounslow and Chepstow-Lusty, 2002).

4. Methodology

Quantitative micro and macrocharcoal content were determined as proxy indicators of fire regimes in the three sections, each of which were freshly prepared in

September 1999. Microcharcoal (mostly <40 μm in particle size) in sediments is often indicative of distal burning, but may mirror local fire activity. However, macrocharcoal content (>125 μm) is a distinct marker of local fire productivity (Clark, 1988; Macdonald et al., 1991). Prior to sampling, the faces were carefully cleaned to remove any loose surface material and cracks within the soil were avoided.

For microcharcoal analysis, 1 cm^3 samples were processed using standard methods for pollen analysis (Berglund, 1986). A known concentration of *Lycopodium* spores were added at the beginning of treatment for assessing microcharcoal concentrations subsequently. Prior to coarse sieving through a 125 μm sieve, the samples were left to stand in a hot water bath of 0.1 m sodium pyrophosphate for 10–20 min. After coarse sieving, the samples were sieved through a 10 μm mesh to remove the clay fraction. The microcharcoal was assessed using the point count method of Clark (1982), where 50 fields of view were examined at a magnification of ×400, using an eye piece graticule.

For macrocharcoal analysis 4 cm^3 of sample was dried in an oven at 105 °C for 6–8 h to remove the water. The samples were then wet sieved at 600, 180 and 125 μm, which removed the clay fraction. The charcoal particles in the size fractions of 600 and 180 μm were counted using a low power stereo microscope. Other observations included noting the presence of fired clay, shell fragments and plant remains. The macrocharcoal content is expressed in particles per cm^3 for these two size fractions. The 125 μm fraction was qualitatively evaluated for evidence of charcoal fragments, but not counted. The two quantitative macrocharcoal values were converted into a single 'equivalent >180 μm macrocharcoal index' in particles/cm^3.

One cm^3 samples were independently taken and heated to 105 °C for 6–8 h to remove the water content and the difference in weight was recorded. Subsequently, organic matter (%OM) was determined by heating to 550 °C for 8 h and measuring the weight loss. Finally, the calcium carbonate content (%$CaCO_3$) was determined by heating the same sample to 950 °C for 8 h and recording further weight loss.

Environmental magnetic measurements (Thompson and Oldfield, 1986) were undertaken on a sub-sample of that used for the microcharcoal analysis. Magnetic susceptibility (χ) was measured using a Bartington MS2 susceptibility meter. This was performed at two frequencies 470 and 4700 Hz to give the low frequency susceptibility (χ_{lf}; Dearing, 1999a), and the percentage frequency dependent susceptibility ($\%\chi_{fd}$). Anhysteretic remanent magnetisations (ARM) were applied using a DC field of 0.1 mT and an alternating field of 80 mT (here termed SARM), and converted to susceptibility of ARM (χ_{ARM}). The ARM was subsequently demagnetised at 40 mT, using static demagnetisation along the ARM axis to give the percentage of ARM remaining (%d.$ARM_{-40\ mT}$). Following saturation isothermal remanent magnetisation (SIRM) at 1 T (using a Newport DC magnet), back field IRM's were applied with a Molspin Ltd Pulse magnetiser at fields of 20, 50 mT, 0.1 and 0.3 T (Thompson and Oldfield, 1986). These IRM values are expressed as the percentage of IRM acquired (%$IRM_{0-20\ mT}$, %$IRM_{0.1-0.3\ T}$ etc. and *S*-ratio; $-IRM_{100\ mT}/SIRM$). Mass specific values were converted to carbonate-free values using the carbonate content. Statistical analyses were performed using SPSS version 10.

5. Results

The details of the environmental interpretation of the post-Roman Geophysics and Causeway Sections are presented elsewhere (Hounslow and Chepstow-Lusty, 2002), but a summary of the relevant data are shown in Table 1. The average micro and macrocharcoal contents of the marsh clays in the Geophysics Section and Causeway Section are quite similar, as are the average organic matter percent and carbonate contents. In contrast, the marsh clays underlying the bath-house structure have distinctly different properties to the other sections (interval A1, Table 1, Fig. 3). At the Bath-house Section, Phase 1 is characterised by microcharcoal contents lower than 0.2 cm^2/cm^3, and low macrocharcoal contents (>180 μm mostly <2 particles/cm^3). The macrocharcoal contents in this phase are still substantially higher than the post-Roman marsh clay in the Geophysics Anomaly Section. The magnetic properties indicate low magnetic concentrations (low χ_{lf}, χ_{ARM}, SIRM; Fig. 3; Table 1), but relatively hard magnetite (high %d.$ARM_{-40\ mT}$).

Phase 3 is characterised by abundant micro and macrocharcoal with microcharcoal abundances exceeding 1 cm^2/cm^3 and organic matter contents in excess of 3% (Fig. 3, Table 1). The high charcoal abundance starts ~14 cm below the floor surface datum of block A, corresponding to the dark soil colour, probably caused by the high abundance of charcoal. Phase 3 is also rich in pink shell fragments (mussels, probably consumed on-site), contributing to a high carbonate content of 16.3%. The high abundance of charcoal in Phase 3, with mussel fragments likely indicates that it may be a mixture of partially burnt charcoal (mixed with ash), with some building and eating debris (i.e. an ash enriched midden). The high microcharcoal content suggests that Phase 3 may represent a final stage in the use of the bath-house as a functional structure. Such use would be compatible with the typical style of late occupation (starting ca. 7th century AD) in the main Butrint site (Hodges et al., 1997). Alternatively, the deposit may represent later (late Byzantine/early medieval?) squatter

Table 1
Mean of magnetic and physical parameters. The intervals in the Bath-house Section are those based on cluster analysis (Fig. 5b)

Section/ Interval	Charcoal		%OM	*%$CaCO_3$	*$\chi_{lf} \times 10^{-7}$ m^3/kg	% χ_{fd}	*$\chi_{ARM} \times 10^{-8}$ m^3/kg	%d_{ARM} −40 mT	χ_{ARM}/SIRM 10^{-3} m/A	%IRM			S-ratio	N
	*Micro cm^2/cm^3	*Macro-particles/cm^3								0–20 mT	0.1–0.3 T	0.3–1 T		
Causeway	0.33	0.23	6.49	13.2	2.28	3.3	53.2	9.6	0.47	29.4	15.7	6.40	1.58	27
Geophysics	0.54	0.37	7.20	10.8	1.73	1.9	26.4	10.2	0.43	26.9	16.0	8.82	1.50	42
Bath-house Section														
B	2.10	34.0	4.02	11.6	4.43	7.8	145.1	5.4	0.45	37.9	10.5	4.99	1.69	15
C	0.50	8.20	3.04	9.60	2.60	3.7	71.6	9.3	0.37	41.7	11.9	3.14	1.70	3
A2	0.80	1.97	3.07	3.97	2.03	3.4	48.0	10.2	0.34	29.1	13.7	7.44	1.58	8
A1	0.20	0.94	2.83	4.32	1.73	2.2	36.2	14.1	0.26	26.7	16.7	6.05	1.55	9

* = $\log_{10}$ Mean. χ_{ARM}, χ_{lf} and SIRM carbonate free mass specific values; %OM = organic matter; N = number of samples.

use of the structure after the bath-house was no longer functional.

The relationship between the charcoal contents and the magnetic parameters were explored by examining the cross correlation between all the physical and magnetic parameters measured (Fig. 4). The most significant cross correlations with micro and macrocharcoal content indicate a number of features:

- micro and macrocharcoal content of the natural marsh clay from all the sections is poorly correlated to all the magnetic parameters, indicating that the magnetic proxies are not responding significantly to changes in fire history in the environment.
- The Bath-house Section samples provide the strongest correlation to the micro and macrocharcoal content. The highest ranking correlations (Pearson correlation coefficient $R > 0.7$) generally involve $\%\chi_{fd}$, χ_{ARM}, $\%IRM_{(0.1–0.3\ T)}$ and organic matter (Fig. 4). The organic matter is most significantly correlated to the micro and macrocharcoal contents only if the bath-house data is included.

Overall the cross-correlations indicate that two magnetic factors are strongly related to the micro or macrocharcoal content:

- Magnetic abundance, expressed particularly by χ_{lf} and χ_{ARM}.
- Magnetic grain size proxies, expressed particularly by $\%\chi_{fd}$, and $\%IRM_{(0.1–0.3\ T)}$, but also sometimes by χ_{ARM}/SIRM (Fig. 4).

Stepwise linear regression was utilised to examine the amount of variance in the charcoal data explained by the magnetics data (input variables transformed to normality if necessary). The macrocharcoal (log transformed) show that χ_{ARM} (log transformed) and $\%\chi_{fd}$ together account for 64% of the variance, with the χ_{ARM} accounting for 95% of this. The microcharcoal data (log transformed) indicate that $\%\chi_{fd}$ and $\%IRM_{(0.1–0.3\ T)}$, account for 68% of the variance, with $\%\chi_{fd}$ accounting for 95% of this. In both cases, the S-ratio shows the next largest correlation to the remaining residuals. Hence, the macrocharcoal data are reflected most strongly in magnetic abundance whereas the microcharcoal is strongly reflected in high contents of superparamagnetic (SP) magnetite. This may indicate that the formation pathways for the amount of magnetite and SP contents of these materials may be related to the degradation or dispersal process of the charcoal.

Multidimensional scaling analysis (MDS) and hierarchical cluster analysis (Rock, 1988) were utilised to examine the sub-division of the Bath-house Section stratigraphy based on the physical properties. Those magnetic parameters identified in Fig. 4 as being most

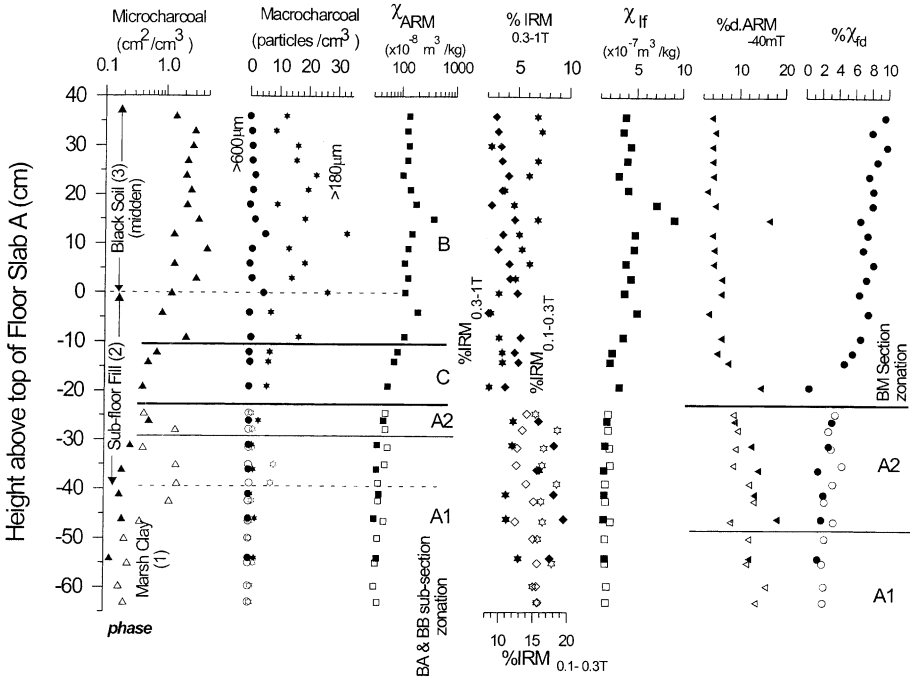

Fig. 3. Summary of the data for the Bath-house Section. Data for the BM sub-section (Fig. 2) are shown as unfilled symbols. The zero cm level is the top of the limestone floor block A (Fig. 2). Stratigraphic phases, are marked as dashed lines and solid lines are stratigraphic sub-divisions based on the multidimensional scaling and cluster analysis (see text). Macrocharcoal, >600 μm (circles), macrocharcoal, >180 μm (stars); $\%IRM_{(0.1\text{–}0.3\ T)}$ (diamonds); $\%IRM_{(0.3\text{–}1\ T)}$ (stars).

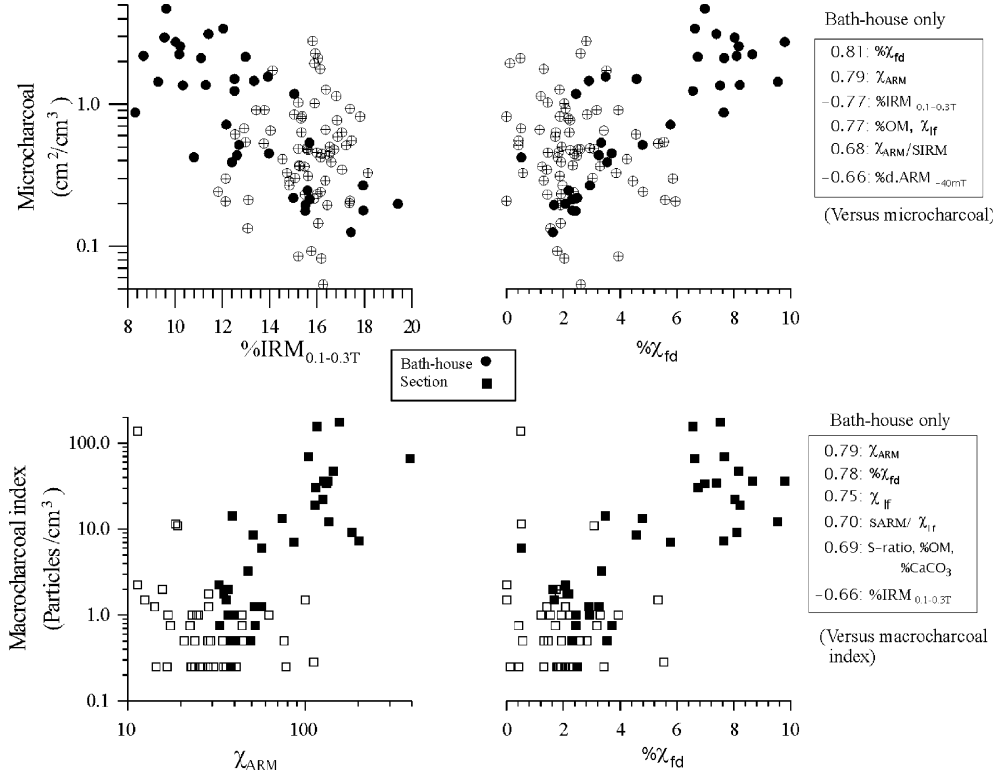

Fig. 4. Summary of relationship between the charcoal contents and magnetic parameters. Pearson correlation coefficients (indicated for $\geqslant 0.66$) for parameters from the Bath-house Section. Unfilled symbols are data from the Geophysics and Causeway Sections.

strongly related to the charcoal content were utilised (i.e. $\%\chi_{fd}$, χ_{lf} $\%IRM_{(0.1–0.3\ T)}$, $\chi_{ARM/}$ SIRM and χ_{ARM}). MDS and cluster analysis were also performed with and without the charcoal content. These show that there are two strong sub-groups of specimens, a Group B rich in charcoal, with high magnetic abundances (Fig. 5; Table 1) and a charcoal poor, Group A. Group A corresponds partly to the marsh clay and partly to the lower part of Phase 2. Including the charcoal data, indicates a 3rd Group C, with Group A sub-divisible into two. These have a clear stratigraphic succession within the section (Fig. 3) indicating a progression from the base (Group A1) to the top (Group B). The same stratigraphic succession is indicated, albeit more weakly in the mineral magnetic data along (Fig. 5). These suggest that the lower part of Phase 2 is partly equivalent to the upper part of sub-section BM, but is partitioned by the wall (Figs. 2 and 3). The low macro and microcharcoal in Group A2 is not suggestive of major wood combustion on the bath-house site in this interval. The high charcoal content of Group B started prior to limestone floor construction, hence it is possible the bath-house went through at least one stage of refurbishment.

The negative relationship (Fig. 4) between charcoal content and $\%IRM_{(0.1–0.3\ T)}$ (or *S*-ratio) appears to be because of the relative enrichment of high coercivity (>100 mT) grains in the marsh clay. There is indication from the larger $\%IRM_{(0.3–1\ T)}$ in the marsh clay (Table 1) that this may be due to elevated haematite (or goethite) content. However, the large $\%IRM_{(0.1–0.3\ T)}$/$\%IRM_{(0.3–1\ T)}$ ratio indicates that a hard magnetite-like phase is also a major contributor to the 0.1–0.3 T coercivity range. The charcoal rich midden deposit (Group B; Table 1) has both enhanced SP magnetite content (i.e. $\%\chi_{fd}$) and enhanced levels of soft magnetite (large $\%IRM_{0–20\ mT}$, low $\%d.ARM_{–40\ mT}$; Table 1). The χ_{ARM}/SIRM values are typical of magnetite grains in the size interval 0.1–0.2 μm (Maher, 1988), therefore the charcoal-related enhancement appears not to be reflected in elevated contents of single domain (SD) magnetite (typically $\chi_{ARM}/SIRM > 0.6 \times 10^{-3}$ m/A), but perhaps pseudo-single domain/multidomain (PSD/MD) magnetite.

6. Discussion

The distinctive feature of the Group B samples is their combination of abundant SP magnetite ($\%\chi_{fd} > 6\%$) and soft magnetite ($\%d.ARM_{–40\ mT} < 10\%$; $\%IRM_{0–20\ mT} > 35\%$). This is also typical of the peat fuel ash residues described by Peters et al. (2000), and the bath-house samples from Phase 3 typically fall within their field of fuel ash residues (Fig. 6). Peters et al. (2000) and Peters et al. (this vol) associate the combination of SP particles and soft magnetite with ultrafine (but magnetically soft remanence) magnetic particles produced during the combustion process. This seems unlikely for the reason that natural chemical processes often lead to grain size populations with distributed tails to grain size ranges. This can be seen in magnetically enhanced soils where high SP magnetite contents are associated with high values of χ_{ARM}/SIRM values ($>0.6 \times 10^{-3}$ m/A) indicating large amounts of SD type grains in addition to SP particles. However, strong SD magnetic signatures are not apparently seen in archaeological fuel combustion residues (e.g. Peters et al., this vol; hearth material, $\chi_{ARM}/SIRM \sim 0.44 \times 10^{-3}$ m/A) or in the data here (Table 1), where room temperature remanence parameters are interpreted to indicate mainly soft, PSD/MD-like and SP magnetite. For comparison, modern combustion of coal and lignites produces no single characteristic magnetic grain size or composition. Instead the type of combustion process, the contaminant mineralogy and

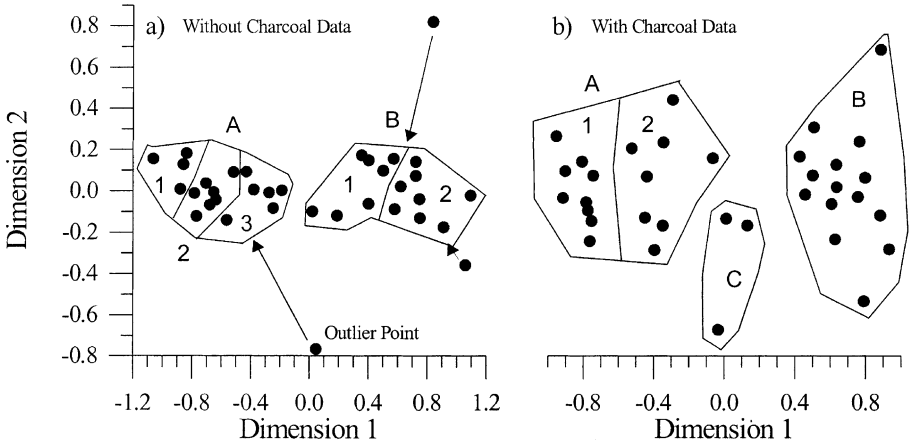

Fig. 5. MDS (two dimensions, variables converted to zero mean, standard deviation of 1.0) using, (a) the magnetics data (parameters used: $^*\chi_{ARM}$, $\%\chi_{fd}$, *S*-ratio, $\%IRM_{(0.1–0.3\ T)}$, $^*\chi_{lf}$). Group memberships of outlier points are indicated with arrows. (b) Analysis using same parameters as (a), but including *microcharcoal, and *macrocharcoal index. Group sub-division is based on hierarchical cluster analysis. In (a) Groups A1+A2 are stratigraphically equivalent to A1 in (b), and B1 + B2 are mostly equivalent to Group B in (b). $^* = \log_{10}$ transformed.

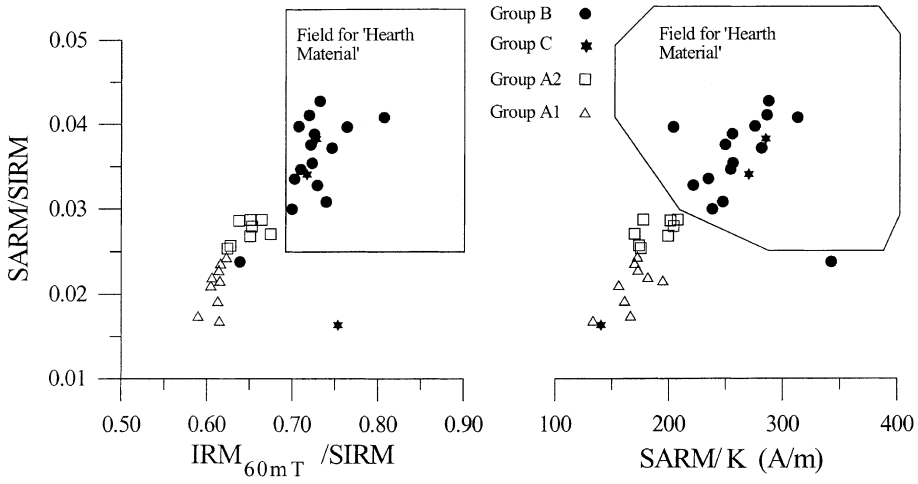

Fig. 6. Comparison of the magnetic parameters from the Bath-house Section with the 'hearth material' data of Peters et al. (2000). Saturation ARM (SARM) of Peters et al. (2000) is based on AF field of 99 mT and DC field of 0.1 mT. $IRM_{(60\ mT)}$ value linearly extrapolated for the bath-house data using $\log_{10}$ of field values.

fuel chemistry dictate the magnetic properties of the fuel ash (Petrovsky and Ellwood, 1999). Hence, the precise combustion mechanisms and the hosts for the magnetite production process need to be better understood to progress the understanding of magnetic measurements of fired archaeological deposits.

Group B samples in comparison to peat ash residues have one to two orders of magnitude lower magnetic abundance (peat: χ_{lf} 10–200 $\times 10^{-7}$ m^3/kg and $\chi_{ARM} \sim$ 1000–9000 $\times 10^{-8}$ m^3/kg; Peters et al., 2000). This can be accounted for by the considerably lower χ_{lf} of wood ash in comparison to peat ash (Peters et al., 2000). The fuel used at the Shën Dëli Roman bath-house would have been charcoal or wood since the Epirus region was important for timber.

7. Conclusions

The charcoal and presumably ash-enriched midden, associated with the Roman bath-house at Shën Dëli, has a distinctive magnetic signature that indicates relatively high abundances of SP magnetic with large amounts of low coercivity magnetite. This apparent bi-modal magnetic grain size population may be a reflection of the combustion process and the nature of the fuel source. The magnetic properties are compatible with a wood or charcoal fuel source.

Acknowledgements

The Butrint Foundation funded part of this work. Sally Martin, Oliver Gilkes, Karen Francis, Aaron Tare and Will Bowden provided logistical assistance.

References

Berglund, B.E., 1986. Handbook of Holocene palaeoecology and palaeohydrology. John Wiley, Chichester.

Chroston, P.N., Hounslow, M.W., 2002. The geophysical survey—the extent and structural layout of the suburbs of Butrint on the Vrina Plain. In: Hodges, R., Bowden, W., Lako, K. (Eds.), Byzantine Butrint, excavations and surveys 1994–99. The British School at Athens, Athens.

Clark, J.S., 1988. Effect of climatic change on fire regimes in northwestern Minnesota. Nature 334, 233–235.

Clark, R.L., 1982. Point count estimation of charcoal in pollen preparations and thin sections of sediments. Pollen et Spores 24, 523–535.

Dearing, J.A., 1999a. Susceptibility. In: Walden, J., Oldfield, F., Smith, J.P. (Eds.), Environmental magnetism: a practical guide. Quaternary Research Association, Cambridge, pp. 35–62.

Dearing, J.A., 1999b. Holocene environmental change from magnetic proxies in lake sediments. In: Maher, B.A., Thompson, R. (Eds.), Quaternary climates, environment and magnetism. Cambridge University Press, Cambridge, pp. 231–278.

Gedye, S.J., Jones, R.T., Tinner, W., Ammann, B., Oldfield, F., 2000. The use of mineral magnetism in the reconstruction of fire history: a case study from Lago di Origlio, Swiss Alps. Palaeogeog. Palaeoclimat. Palaeocol 164, 101–110.

Hodges, R, Saraci, G., Bowden, W., Chiles, P., Gilkes, O., Lako, K., Lane, A., Martin, S., Mitchell, J., Moreland, J., O'Hara, S., Pluciennik, M., Watson, L., 1997. Late-antique and Byzantine Butrint: interim report on the port and its hinterland (1994–95). J. Roman Archaeology 10, 207–234.

Hodges, R., Bowden, W., Lako, K., 2002. Byzantine Butrint, excavations and surveys 1994–99. The British School at Athens, Athens.

Hounslow, M.W., Chepstow-Lusty, A., 2002. Environmental events at Butrint over the last 3500 years: A preliminary investigation of fire history, sedimentological changes and archaeomagnetic dating. In: Hodges, R., Bowden, W., Lako, K. (Eds.), Byzantine Butrint, excavations and surveys 1994–99. The British School at Athens, Athens.

Ketterings, Q.M., Bigham, J.M., Laperche, V., 2000. Changes in soil mineralogy and texture caused by slash and burn fires in Sumatra. Indonesia. Soil. Sci. Soc. Am. Hour 64, 1108–1117.

Kletetschka, G., Banerjee, S.K., 1995. Magnetic stratigraphy of Chinese loess as a record of natural fires. Geophys. Res. Lett. 22, 1341–1343.

Lu, H., Zhou, L., Han, J., Wu, N., Liu, T., Gu, Z., Liu, B., 2000. Effect of burning C3 and C4 plants on the magnetic susceptibility signals in soils. Geophys. Res. Lett. 27, 2031–2036.

Macdonald, G.M., Larsen, C.P.S., Szeicz, J.M., Moser, K.A., 1991. The reconstruction of boreal forest fire history from lake sediments: a comparison of charcoal, pollen, sedimentological and geochemical indices. Quater. Sci. Rev. 10, 53–71.

Maher, B.A., 1988. Magnetic properties of some synthetic sub-micron magnetites. Geophys. J. 94, 83–96.

Mathers, S., Brew, D.S., Arthurton, R.S., 1999. Rapid Holocene evolution and neotectonics of the Albanian Adriatic coastline. J. Coastal Res. 15, 345–354.

Patterson, W.A., Edwards, K.J., McGuire, D.J., 1987. Microscopic charcoal as a fossil indicator of fire. Quater. Sci. Rev. 6, 3–23.

Peters, C., Church, M.J., Coles, G., 2000. Mineral magnetism and archaeology at Galson on the Isle of Lewis. Scotland Phys. Chem. Earth (A) 25, 455–460.

Peters, C., Thompson, R., Harrison, A., Church, M.J. Low temperature magnetic characterisation of fire ash residues. Phys. Chem. Earth. (A) this vol.

Petrovsky, E., Ellwood, B.B., 1999. Magnetic monitoring of air land and water pollution. In: Maher, B.A., Thompson, R. (Eds.), Quaternary climates, environment and magnetism. Cambridge University Press, Cambridge, pp. 279–322.

Reale, O., Dirmeyer, P., 2000. Modelling the effects of vegetation on the Mediterranean climate during the Roman classical period, Part I: Climate history and model sensitivity. Global Planet. Change 25, 163–184.

Rock, N.M.S., 1988. Numerical geology. In: Bhattacharji, S., Friedman, G.M., Neugebauer, H.J., Seilacher, A. (Eds.), Lecture notes in the earth sciences, vol. 18. Springer-Verlag, Berlin.

Rummery, T.A., 1983. The use of magnetic measurements in interpreting the fire histories of lake drainage basins. Hydrobiologica 103, 53–58.

Schmidt, M.W.I., Skjemstad, J.O., Gehrt, E., Kogel-Knabner, I., 1999. Charred organic carbon in German Cherozemic soils. Eur. J. Soil Sci. 50, 351–365.

Thompson, R., Oldfield, F., 1986. Environmental magnetism. Allen & Unwin, London.